XLVI CILAMCE
VITÓRIA - ES - BRAZIL - 2025
XLVI IBERO-LATIN AMERICAN CONGRESS ON COMPUTATIONAL METHODS IN ENGENEERING

Topology Optimization of Undamped Plates for the Maximization of the Fundamental Frequency

Matheus Fabbris Guerreiro[1], Jucélio Tomás Pereira[1], Jéderson da Silva[2], João Luiz do Vale[2]

[1]*Laboratory of Computational Solid Mechanics, Postgraduate Program in Mechanical Engineering (PG-Mec), Federal University of Paraná*
Polytechnic Center, 81530-000, Curitiba, Brazil
matheus.fabbris@gmail.com, jucelio.tomas@ufpr.br
[2]*Department of Mechanical Engineering, Federal University of Technology of Paraná*
Av. João Miguel Caram, 731, 86036-700, Londrina, Brazil
jedersonsilva@utfpr.edu.br, joaovale@utfpr.edu.br

Abstract. In mechanical systems subjected to dynamic loads, resonance may occur when one of the structure's natural frequencies coincides with its operating range, potentially compromising structural integrity. In response, this work presents a topology optimization scheme to maximize the fundamental natural frequency of undamped plate-type structures. To address this, an optimization problem is formulated using the Solid Isotropic Material with Penalization (SIMP) method, under a volume constraint. Two auxiliary functionals are incorporated into the objective function: one penalizes intermediate density regions, and the other penalizes the density gradient to mitigate checkerboard patterns, promote smoother boundaries and mesh independency. This regularization strategy enhances the quality and robustness of the final topological layout. The problem is solved via the Augmented Lagrangian Method, ensuring stable convergence. The methodology is applied to two benchmark cases from the literature, and a mesh-dependence analysis is conducted to evaluate solution robustness. Results demonstrate that the proposed approach effectively increases the fundamental frequency and produces smooth, well-defined topologies without checkerboard patterns. These characteristics contribute to more reliable designs, with improved dynamic behavior and extended service life.

Keywords: Topology optimization, SIMP, intermediate density, checkerboard, plates

1 Introduction

Topology optimization is one of the main tools used in the design of more efficient structural components, especially in applications subjected to dynamic loads, such as in the aerospace, automotive, and aeronautical industries (Zhu et al. [1]). In these contexts, the occurrence of resonance can compromise structural integrity and significantly reduce the service life of components. Therefore, maximizing the fundamental natural frequency emerges as a relevant strategy to shift the first vibrational mode away from the operating frequency ranges of the structures, reducing the risk of resonance in mechanical components.

Among topology optimization methods, those based on microstructures stand out. In particular, the Solid Isotropic Material with Penalization (SIMP) method is widely used in structural optimization problems and allows for a continuous variation of the relative densities of the elements, unlike other methods that produce binary results (Bendsoe and Sigmund [2]). Among the studies focused on natural frequency optimization, the work of Du and Olhoff [3] is a key reference. They proposed a formulation using the SIMP method to maximize natural frequency ranges in continuous structures, including different geometries and boundary conditions, with emphasis on beams and plates. To represent plate geometries, the authors employed a three-dimensional discretization with hexahedral elements. Although they achieved significant increases in natural frequencies, the final results exhibited were poorly defined and presents jagged boundaries, along with regions of intermediate densities, which may affect the interpretability and practical application of the obtained topologies. To mitigate issues such as checkerboard patterns and mesh dependency, the authors employed a mesh-independent sensitivity filter, as proposed in Sigmund and Petersson [4].

Several strategies have been developed in the literature to overcome limitations associated with the traditional method. For instance, Bogomolny [5] proposed a topology optimization approach focused on natural frequencies,

using Combined Approximations to reduce the computational cost associated with repeated eigenvalue problem solutions. His study considered 2D and 3D cases for maximizing eigenvalues and eigenvalue gaps. Although focused on numerical efficiency, his work reinforces the relevance of frequency maximization problems within the context of topology optimization.

Other approaches seek to directly control the vibration modes of structures. Tsai and Cheng [6] used the SIMP method to maximize the fundamental frequency and introduced weighted constraints during the iterative process to avoid mode switching, applying the Modal Assurance Criterion to identify the target modes. In an even more direct approach, Li et al. [7] developed a differentiable function that enables imposing constraints on displacements and stresses associated with the fundamental mode, even in the presence of repeated eigenvalues. Despite their merits, these approaches tend to increase the computational complexity of the problem.

In an industrial context, Bacciaglia et al. [8] proposed a methodology based on voxelization and the Bidirectional Evolutionary Structural Optimization Method to optimize the fundamental natural frequency of complex three-dimensional structures, incorporating a connectivity verification algorithm to ensure manufacturability. Their work highlights the limitations of classical topology optimization methods for the intended application and reinforces the importance of complementary constraints to achieve satisfactory results.

In this context, the present work proposes a formulation for maximizing the fundamental frequency of plates using the SIMP method with a volume constraint, complemented by two auxiliary functionals. The first penalizes regions with intermediate densities, and the second acts on the density gradient field, promoting smoother boundaries and mitigating the formation of checkerboard patterns. The methodology is applied to two benchmark cases from the literature. The robustness of the solutions is verified through a mesh-dependence analysis, and the gains in fundamental frequency are quantified, demonstrating the potential of the proposed approach.

2 Problem Formulation and Methodology

This work considers a 2D undamped plate-type structure composed of a linear, homogeneous, and isotropic elastic material. The mechanical behavior of the plate is described using the First-Order Shear Deformation Theory, also known as Reissner–Mindlin plate theory, which accounts for transverse shear deformation (Mindlin [9]). The domain is discretized using quadrilateral finite elements with four nodes (Q4).

The design variables of the topology optimization problem are defined nodally as relative material densities. However, for the evaluation of the elementary density used in the interpolation of material properties, the density field is sampled at the centroid of each finite element.

2.1 Modal Analysis and Formulation

The analysis is conducted through a generalized eigenvalue problem derived from the free vibration formulation. The resulting matrix equation for this problem is:

$$\mathbf{K}(\boldsymbol{\rho})\,\mathbf{u}_j = \lambda_j\,\mathbf{M}(\boldsymbol{\rho})\,\mathbf{u}_j, \quad \text{subject to} \quad \mathbf{u}_j^T\mathbf{M}(\boldsymbol{\rho})\mathbf{u}_j = 1, \tag{1}$$

where $\mathbf{K}(\boldsymbol{\rho})$ and $\mathbf{M}(\boldsymbol{\rho})$ are the global stiffness and mass matrices, respectively, dependent on the relative density distribution $\boldsymbol{\rho} = \{\rho_1, \ldots, \rho_{N_e}\}$ over the finite elements, with N_e being the total number of elements. The eigenvalues $\lambda_j = \omega_j^2$ correspond to the squares of the structure's natural frequencies, and $\mathbf{u}_j$ is the associated eigenvector.

2.2 Material Interpolation via SIMP

The interpolation of material properties is done using the SIMP model, as presented by Bendsoe and Sigmund [2]. Assuming a piecewise constant density per finite element, the global stiffness and mass matrices of the system are defined as

$$\mathbf{K}(\boldsymbol{\rho}) = \sum_{e=1}^{N_e} \rho_e^p\,\mathbf{K}_e^0, \quad \text{and} \quad \mathbf{M}(\boldsymbol{\rho}) = \sum_{e=1}^{N_e} \rho_e^q\,\mathbf{M}_e^0, \tag{2}$$

where $\mathbf{K}_e^0$ and $\mathbf{M}_e^0$ are the elementary reference stiffness and mass matrices (assuming fully solid material), $\rho_e \in [\rho_{\min}, 1]$ is the relative density of element e, with $\rho_{\min} = 0.01$ to ensure that all elements keep minimal stiffness

and mass, maintaining numerical stability throughout the optimization process, and p and q are the penalization exponents for stiffness and mass, respectively. In this study, $p = 3$ is adopted, a value which is commonly used in the literature, and q is defined as 1 for $\rho_e > 0.1$ and $q = 6$ for $\rho_e \leq 0.1$, a greater value than p in order to avoid localized vibration modes as suggested by Pedersen [10].

2.3 Proposed Optimization Problem

The objective of the optimization problem is to determine the optimal material distribution that maximizes the smallest non-zero natural frequency of the structure (fundamental frequency), λ_1. The design variables are the relative densities $\boldsymbol{\rho} = \{\rho_1, \ldots, \rho_{N_e}\}$.

An equality-type volume constraint h_V is imposed on the problem, meaning that the final material volume must match a specified fraction $\alpha \in (0, 1]$ of the total domain volume $V_0 = Ah$, where A is the plate area and h is its thickness.

The optimization problem can then be stated in standard form as, where A_e is the area of element e,

$$\begin{aligned} \min \quad & -\lambda_1(\boldsymbol{\rho}) \\ \text{subject to} \quad & \mathbf{K}(\boldsymbol{\rho})\,\mathbf{u}_j = \lambda_j\,\mathbf{M}(\boldsymbol{\rho})\,\mathbf{u}_j, \\ & \mathbf{u}_j^T\mathbf{M}(\boldsymbol{\rho})\mathbf{u}_j = 1, \\ & h_V(\boldsymbol{\rho}) = \frac{V(\boldsymbol{\rho})}{\alpha V_0} - 1 = 0, \text{ with } V(\boldsymbol{\rho}) = \sum_{e=1}^{N_e} \rho_e A_e h, \\ & \rho_{\min} \leq \rho_e \leq 1, \quad \forall\, e = 1, \ldots, N_e. \end{aligned} \tag{3}$$

2.4 Additional Penalization Functionals

To reduce intermediate-density (gray) regions, obtain solutions with better-defined boundaries, and mitigate the checkerboard effect, two penalization functionals based on the works of Pereira et al. [11] and da Silva et al. [12] are added to the objective function.

The first functional, denoted by $F_m(\rho)$, aims to penalize the presence of intermediate-density regions, favoring material distributions closer to the extremes (0 or 1). This functional is defined as

$$F_m(\rho) = \int_\Omega \rho\,(1-\rho)\; d\Omega, \tag{4}$$

where ρ represents the relative density field over the domain Ω.

The second functional, $F_\rho(\rho)$, acts as a regularization term, penalizing abrupt changes in the density field. Its goal is to suppress unwanted mesh patterns such as the checkerboard effect and promote smoother boundaries between material and void regions. This functional is defined as

$$F_\rho(\rho) = \int_\Omega \nabla\rho^T \nabla\rho\, d\Omega, \tag{5}$$

where $\nabla\rho$ is the gradient of the density field.

Both functionals are weighted by positive scalar coefficients, r_m and r_ρ, which control their relative influence in the objective function. The new scalar objective function to be minimized becomes

$$F(\rho) = -\lambda_1(\rho) + r_m F_m(\rho) + r_\rho F_\rho(\rho), \tag{6}$$

where the two additional terms act as penalizations added to the fundamental natural frequency. The values of r_m and r_ρ are chosen to ensure consistent order of magnitude and units between the terms and to maintain controlled influence during the optimization process.

2.5 Solution via Augmented Lagrangian Method

The proposed optimization problem is solved using the Augmented Lagrangian Method (ALM), a widely adopted approach in optimization due to its good numerical stability (Arora [13]). The Augmented Lagrangian functional associated with the problem is defined as

$$L_A(\rho, \eta_k, r_k) = F(\rho) + \eta_k \, h_V(\rho) + r_k \, h_V(\rho)^2, \tag{7}$$

where η_k is the Lagrange multiplier associated with the constraint and $r_k > 0$ is the quadratic penalty parameter.

At each optimization iteration, the function L_A is minimized with respect to ρ using its gradient. After each minimization step, the values of η_k and r_k are updated based on the constraint violation. This iterative scheme ensures that the final solution satisfies the volume constraint accurately.

2.6 Sensitivity Analysis

To define the sensitivity of the augmented Lagrangian functional with respect to the design variables ρ_e, it is necessary to compute the partial derivatives of each term in the objective function and the volume constraint.

Assuming that the eigenvalue λ_1 is simple (i.e., not repeated) and that the associated eigenvector is normalized according to eq. (1), the total sensitivity of the augmented Lagrangian functional with respect to the relative density of element e is

$$\frac{\partial L_A}{\partial \rho_e} = -\frac{\partial \lambda_1}{\partial \rho_e} + r_m \frac{\partial F_m}{\partial \rho_e} + r_\rho \frac{\partial F_\rho}{\partial \rho_e} + \eta_k \frac{\partial h_V}{\partial \rho_e} + 2 r_k h_V(\rho) \frac{\partial h_V}{\partial \rho_e}. \tag{8}$$

More details on the sensitivities of the eigenvalue problem can be found in Du and Olhoff [3], while the sensitivities of the functionals F_m and F_ρ, associated with the penalty terms, are presented in Pereira et al. [11] and da Silva et al. [12]. The sensitivity of the total volume is obtained by differentiating h_V with respect to ρ_e which is equal to $A_e h$.

3 Case Studies

The choice of study cases and the application of a mesh dependency analysis were guided by best practices in topology optimization, as discussed by Sigmund [14]. According to the author, clarity in problem definition, the use of benchmark examples from the literature, and the objective assessment of results are key aspects to ensure reproducibility and credibility in this field.

Two topology optimization cases for plates were selected to validate the proposed methodology, both originally presented by Du and Olhoff [3]. The geometry consists of a square plate with dimensions $20 \times 20\,\mathrm{m}$ and a constant thickness of $1\,\mathrm{m}$, subject to a volume constraint of 50% ($\alpha = 0.5$). The mechanical properties are a Young's modulus $E = 10^{11} Pa$, a Poisson's ratio $\nu = 0.3$ and a mass density $\rho_{md} = 7800\ kg/m^3$.

In both cases, a concentrated mass equivalent to 10% of the total mass of the original plate is added. This mass is incorporated directly into the global mass matrix, distributed over the elements corresponding to the region of influence. The plate is modeled using two-dimensional four-node quadrilateral finite elements.

The two analyzed cases are:

- **Case A:** all edges clamped and a concentrated mass placed at the center of the plate;
- **Case B:** one edge clamped and a concentrated mass placed at the center of the opposite edge.

For both cases, a uniform mesh with 60×60 elements is adopted.

The calibration of the proposed method's parameters followed a logical sequence. First, analyses were performed varying the parameter r_k, responsible for enforcing the volume constraint, until a satisfactory convergence behavior was achieved. Next, the parameter r_ρ was defined to mitigate the checkerboard effect and smooth the material boundaries. Finally, the parameter r_m was adjusted to penalize intermediate densities.

In addition to the main analysis, a mesh dependency study was later conducted by comparing the results obtained with a refined mesh of 80×80 elements.

Numerical analyses for each case are presented in the next section, including the obtained values for the fundamental natural frequency, the functional terms, and visualizations of the final topologies.

4 Results and Discussion

This section presents the results for the two cases. The analyses include the optimal material distribution, fundamental natural frequency values, auxiliary functionals, objective function evolution, the influence of additional functionals on convergence, the resulting topology patterns, and the mesh dependency assessment.

4.1 Case A

The first step consisted of defining the parameter r_k, which is responsible for enforcing the volume constraint. After preliminary testing, $r_k = 10$ was adopted. Subsequently, analyses were carried out by first varying the value of r_ρ, followed by tests with different values of r_m. The final topologies obtained with $r_\rho = 1,\ 5,$ and 10 combined with $r_m = 10,\ 30,$ and 50 are shown in Fig. 1.

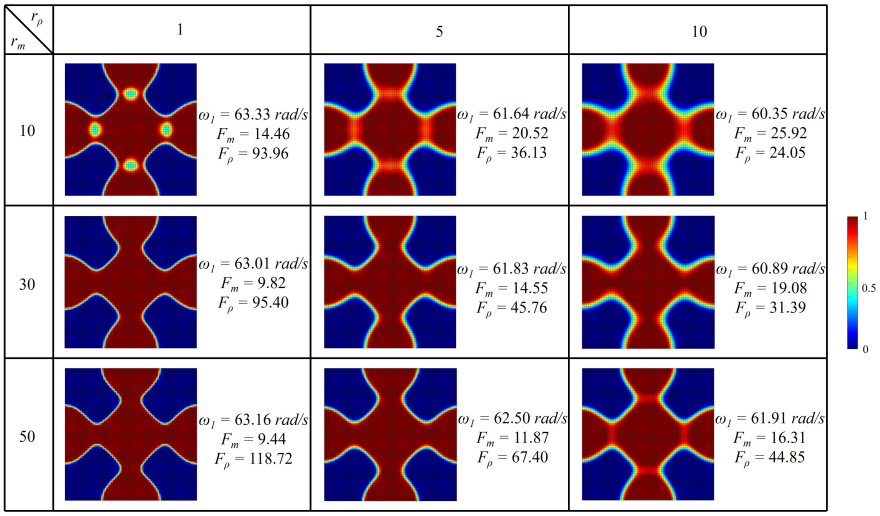


Figure 1. Results of Case A analysis with variation of r_m and r_ρ, with $r_k = 10$.

It can be observed that for $r_m = 10$, regions with intermediate densities and poorly defined boundaries appear, even with higher r_ρ. Increasing r_m to 30 and 50 reduces these regions, yielding topologies with sharper material–void transitions. For $r_m = 50$, the topology stabilizes for both $r_\rho = 1$ and 5.

To assess the robustness of the solutions obtained, a mesh dependency analysis was performed, presented in Fig. 2, for three combinations of penalization: without auxiliary functionals ($r_m = r_\rho = 0$), $r_m = 50,\ r_\rho = 1$, and $r_m = 50,\ r_\rho = 5$, using meshes of 60×60 and 80×80 elements.

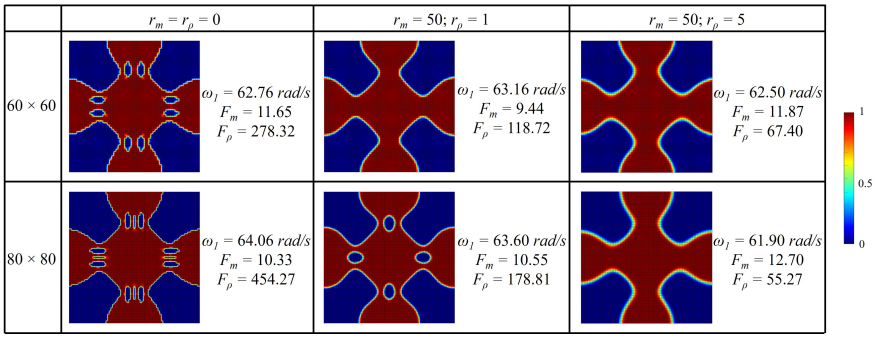


Figure 2. Case A mesh dependency analysis for different pairs of r_ρ and r_m, with 60×60 and 80×80 meshes.

In the unpenalized case, distinct checkerboard patterns are observed between the two meshes, indicating a strong dependence on discretization. For the initially considered satisfactory combination, $r_m = 50$ and $r_\rho = 1$, mesh refinement resulted in the reappearance of checkerboard patterns, indicating that the value of r_ρ was

insufficient to ensure robustness for finer discretizations. When increasing r_ρ to 5, the final topology remained stable between both meshes, with no checkerboard effect, characterizing numerical mesh independence. With that, the regularization adopted in this work proved to be effective, as also observed in Pereira et al. [11] and da Silva et al. [12], ensuring clearer topologies and suppressing numerical instabilities.

In addition to the observed numerical robustness, a significant increase in the fundamental natural frequency throughout the optimization process is also highlighted. The initial value of $\omega_1 = 30.21$ rad/s was increased to $\omega_1 = 61.90$ rad/s, which represents an increase of 105% in the final configuration with refined mesh, showing a substantial gain in the dynamic stiffness of the structure.

Moreover, the optimized layouts resemble the geometries found in Du and Olhoff [3], reinforcing the validity of the proposed formulation and consistency with other studies.

To complement the analysis, Fig. 3 presents the evolution of the eigenvalues and the volume constraint obtained throughout the optimization process. The results refer to the refined mesh of 80×80 elements and the penalization parameters $r_m = 50$ and $r_\rho = 5$. The first graph indicates the absence of bimodality in the fundamental frequency, while the second confirms the consistent satisfaction of the volume constraint, validating the assumptions adopted in the formulation.

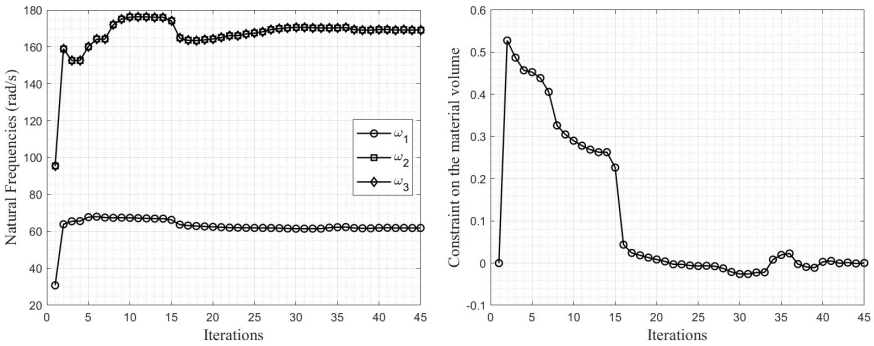


Figure 3. Case A evolution of natural frequencies during optimization (left) and volume constraint (right).

4.2 Case B

Following the same methodology adopted in the previous case, tests were carried out by varying the penalization parameters r_m and r_ρ, with the value of r_k fixed at 50. Figure 4 presents the mesh dependency analysis for the case without penalization and for the final result obtained with mild penalization, using $r_m = 0.1$ and $r_\rho = 0.01$.

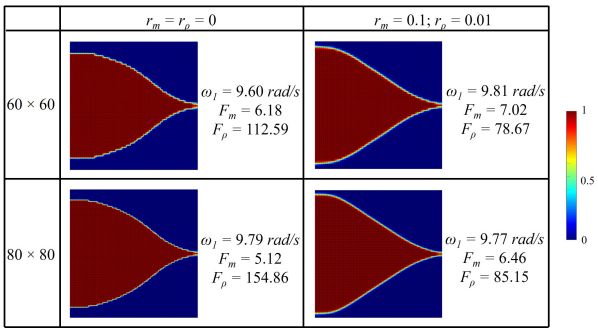


Figure 4. Case B mesh dependency analysis, with and without penalization.

It is observed that in the absence of auxiliary functionals, mesh refinement leads to a sharp increase in the value of F_ρ, indicating greater oscillation in the density field and a dependence on discretization. With the adopted penalization, the topology remains virtually unchanged between the two meshes, with low variation in the values of F_m and F_ρ, demonstrating mesh independence and greater solution robustness.

Similar to Case A, the adopted methodology also resulted in a substantial increase in the fundamental frequency. The initial value of $\omega_1 = 3.45$ rad/s was increased to $\omega_1 = 9.77$ rad/s, a 183% growth, highlighting the potential of the proposed formulation for applications where resonance avoidance is critical.

5 Conclusions

This work presented a topology optimization formulation aimed at maximizing the fundamental natural frequency of plates. For that purpose, the SIMP method with a volume constraint was adopted, complemented by two auxiliary functionals: one focused on penalizing regions with intermediate densities and another on penalizing the density gradient, aiming to smooth structural boundaries and mitigate the checkerboard effect.

The methodology was applied to two classic cases from the literature with different boundary conditions. In both cases, the fundamental frequency was significantly increased, highlighting the potential of the proposed approach to enhance the dynamic stiffness of vibrating structures.

The proposed functionals proved effective in improving topology quality and ensure mesh independency. The gradient penalization was essential to suppress checkerboard patterns, while the penalization of intermediate densities contributed to sharper boundaries without compromising convergence. The results remained stable even with mesh refinement.

As future work, the methodology could be applied to more complex geometries and extended to higher-order natural frequencies, as well as to the maximization of eigenvalue gaps.

Acknowledgements. The authors gratefully acknowledge the support of the Postgraduate Program in Mechanical Engineering (PG-Mec) at the Federal University of Paraná (UFPR). This study was financed in part by the Coordenação de Aperfeiçoamento de Pessoal de Nível Superior - Brasil (CAPES) - Finance Code 001.

Authorship statement. The authors hereby confirm that they are the sole liable persons responsible for the authorship of this work, and that all material that has been herein included as part of the present paper is either the property (and authorship) of the authors, or has the permission of the owners to be included here.

References

[1] J. Zhu, W. Zhang, and L. Xia. Topology optimization in aircraft and aerospace structures design. *Archives of Computational Methods*, vol. 23, pp. 595–622, 2016.

[2] M. P. Bendsoe and O. Sigmund. *Topology Optimization: Theory, Methods and Applications*. Springer, 2 edition, 2004.

[3] J. Du and N. Olhoff. Topological design of freely vibrating continuum structures for maximum values of simple and multiple eigenfrequencies and frequency gaps. *Structural and Multidisciplinary Optimization*, vol. 34, pp. 91–110, 2007.

[4] O. Sigmund and J. Petersson. Numerical instabilities in topology optimization: A survey on procedures dealing with checkerboards, mesh-dependencies and local minima. *Structural and Multidisciplinary Optimization*, vol. 16, pp. 68–75, 1998.

[5] M. Bogomolny. Topology optimization for free vibrations using combined approximations. *International Journal for Numerical Methods in Engineering*, vol. 82, n. 5, pp. 617–636, 2009.

[6] T. Tsai and C. Cheng. Structural design for desired eigenfrequencies and mode shapes using topology optimization. *Structural and Multidisciplinary Optimization*, vol. 49, pp. 673–686, 2013.

[7] B. Li, Y. Fu, and G. J. Kennedy. Topology optimization using an eigenvector aggregate. *Structural and Multidisciplinary Optimization*, vol. 66, n. 221, 2023.

[8] A. Bacciaglia, A. Ceruti, and A. Liverani. Voxel-based evolutionary topological optimization of connected structures for natural frequency optimization. *International Journal of Mechanics and Materials Design*, vol. 20, pp. 1209–1228, 2024.

[9] R. Mindlin. Influence of rotatory inertia and shear on flexural motions of isotropic, elastic plates. *J. Appl. Mech.*, vol. 18, n. 1, pp. 31–38, 1951.

[10] N. L. Pedersen. Maximization of eigenvalues using topology optimization. *Structural and Multidisciplinary Optimization*, vol. 20, pp. 2–11, 2000.

[11] J. T. Pereira, E. A. Fancello, and C. S. Barcellos. Topology optimization of continuum structures with material failure constraints. *Structural and Multidisciplinary Optimization*, vol. 26, pp. 50–66, 2004.

[12] J. da Silva, J. T. Pereira, and D. A. F. Torres. h-adaptive topology optimization considering variations of material properties and energy error density recovery. *Engineering Computations 37(9):3209-3241*, vol. 37, n. 9, pp. 3209–3241, 2020.

[13] J. Arora. *Introduction to Optimum Design*. Elsevier, 4 edition, 2017.

[14] O. Sigmund. On benchmarking and good scientific practise in topology optimization. *Structural and Multidisciplinary Optimization*, vol. 65, n. 315, 2022.